

CONF-960465--1

SAND095-2936C

RING-FIELD EUVL CAMERA WITH LARGE ETENDU

W. C. Sweatt  
Sandia National Laboratories  
Albuquerque, NM, 87185-0980  
WSWEATT@SANDIA.GOV

RECEIVED  
JAN 16 1996  
OSTI

**ABSTRACT:** These scanning cameras with large instantaneous fields make efficient use of the new, 300- $\mu$ m diameter, debris-less laser-plasma sources while printing 100-nm features.

**DISCLAIMER**

This report was prepared as an account of work sponsored by an agency of the United States Government. Neither the United States Government nor any agency thereof, nor any of their employees, makes any warranty, express or implied, or assumes any legal liability or responsibility for the accuracy, completeness, or usefulness of any information, apparatus, product, or process disclosed, or represents that its use would not infringe privately owned rights. Reference herein to any specific commercial product, process, or service by trade name, trademark, manufacturer, or otherwise does not necessarily constitute or imply its endorsement, recommendation, or favoring by the United States Government or any agency thereof. The views and opinions of authors expressed herein do not necessarily state or reflect those of the United States Government or any agency thereof.

DISTRIBUTION OF THIS DOCUMENT IS UNLIMITED

MASTER

# RING-FIELD EUVL CAMERA WITH LARGE ETENDU

W. C. Sweatt  
Sandia National Laboratories  
Albuquerque, NM, 87185-0980  
WSWEATT@SANDIA.GOV

## SUMMARY

**INTRODUCTION:** A "debris-less" laser-plasma source (LPS) of extreme-UV radiation has been developed by Kubiak, et al.<sup>1</sup>. This is a huge step forward for the extreme-UV lithography program (EUVL) because it will extend the life of the collecting mirrors that face the source. This source has a 300- $\mu\text{m}$  diameter ( $D_{\text{source}}$ ) which is larger than the earlier, ~75- $\mu\text{m}$  diameter plasma balls created on metal targets. The larger source size requires that the Etendu of the system must also be larger if the source radiation is to be used efficiently.

A family of 4-mirror, scanning, ring-field lithography cameras has been designed that can be efficiently coupled to a "debris-less" LPS. The most promising design has a 0.085-numerical aperture ( $na_{\text{camera}}$ ) for printing  $\approx$ 100-nm features. At the image plane it has 13 nm of distortion and a 98% Strehl ratio across its 7-mm wide ring-field ( $\Delta r$ ).

**CAMERA EFFICIENCY:** A camera's thru-put is a function of its Etendu, defined as:

$$E_{\text{camera}} = na_{\text{camera}} \cdot \Delta r \quad (1)$$

Not surprisingly, the condenser efficiency is limited by the maximum camera thru-put. The optimal condenser Etendu,  $E_{\text{condenser}}$ , is equal to the product of the camera Etendu and the partial coherence fill factor,  $\sigma \approx 60\%$  (Kohler illumination):

$$E_{\text{condenser}} = E_{\text{camera}} \cdot \sigma \quad (2)$$

The condenser Etendu can be defined at the source as:

$$E_{\text{condenser}} = D_{\text{source}} \cdot \theta_{\text{condenser}} \quad (3)$$

where  $\theta_{\text{condenser}}$  is the collection half-angle. Combining equations (1), (2), and (3) relates the collection angle, and hence, efficiency to the ring-field width:

$$\theta_{\text{condenser}} = na_{\text{camera}} \cdot \Delta r / D_{\text{source}} \quad (4)$$

From this, the collection solid angle and the collection efficiency can be calculated. High efficiency condensers have been designed<sup>2</sup> that use critical illumination in the scanning direction. These designs have larger collection angles in the sagittal direction but their collection angle in the tangential direction is still limited by Equation (4).

**PREVIOUS SCANNING, RING-FIELD CAMERAS:** Scanning, ring-field cameras<sup>3,4</sup> have been designed for use with high brightness sources such as synchrotrons and metal-foil laser-plasma sources. Unfortunately, when used with one of the 300- $\mu\text{m}$  diameter debris-less sources, the small Etendus of these cameras [ $E_{\text{camera}}=0.1 \text{ mm-sr}$ ] can only use an F/2.5 collector mirror ( $\theta_{\text{condenser}}=0.2$ ). This only collects 1% of the EUV and a high efficiency condenser<sup>2</sup> can only collect  $\approx 4.5\%$ .

To make better use of the radiation from a debris-less source, the ring-field width must be widened to increase the camera's Etendu (increasing  $na_{\text{camera}}$  is much harder). Unfortunately,

neither of the previous designs<sup>3,4</sup> can be widened enough to be usable. In the Jewell-Thompson camera<sup>3</sup> (Figure 1) the imagery is good across a small ( $\Delta r=1$  mm) ring-field width. However the large chief ray angles cause the field-dependent aberrations to degrade significantly with small changes in field height.

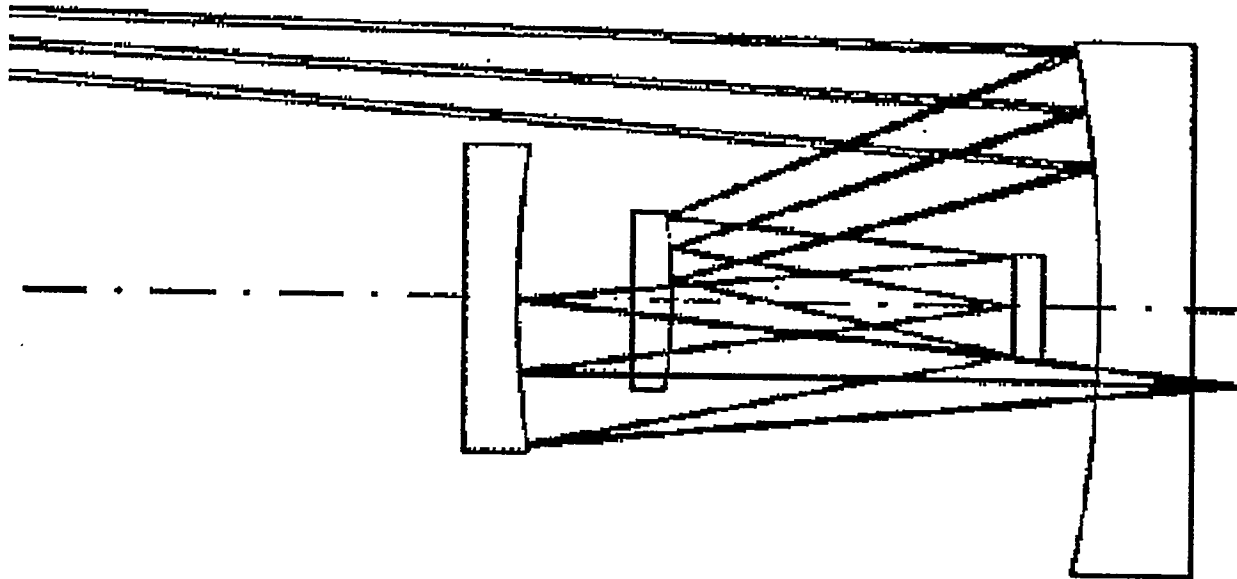


Figure 1. Jewell-Thompson camera.

The "reflective triplet" of Bruning, et. al.<sup>4</sup> (Figure 2) has an inaccessible aperture stop; that is, a hard stop located where the chief ray crosses the axis between mirrors M2 and M3 will vignette the beam reflected off mirror M3. For modest ring-field widths,  $\Delta r \approx 1$  mm, a set of partial apertures located on mirrors M2 and M3, and at the true stop position give acceptable imagery. Wider ring fields allow unacceptable imagery variations across the field.

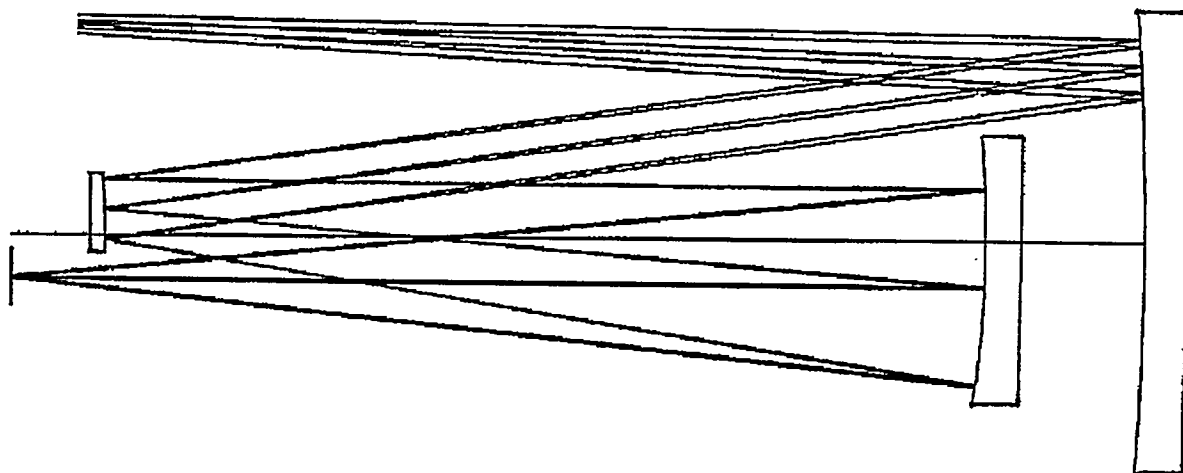


Figure 2. Bruning, et. al. camera.

**LARGE ETENDU SCANNING RING-FIELD CAMERAS:** A type of new, large Etendu camera designs have Etendus more than twice as large as those listed above. As shown in Figure 3, the new design is similar to Bruning's triplet, except that a weakly powered mirror has been added following Mirror M1. As with the triplet, it uses a partial stop and apertures to limit the beam size. However, there is access to the bottom and sides of the beam at the ideal stop location. Two additional apertures, shown in Figure 3, are used to trim the beam's top. This family of cameras has essentially invariant imagery over a fairly wide ring-field.

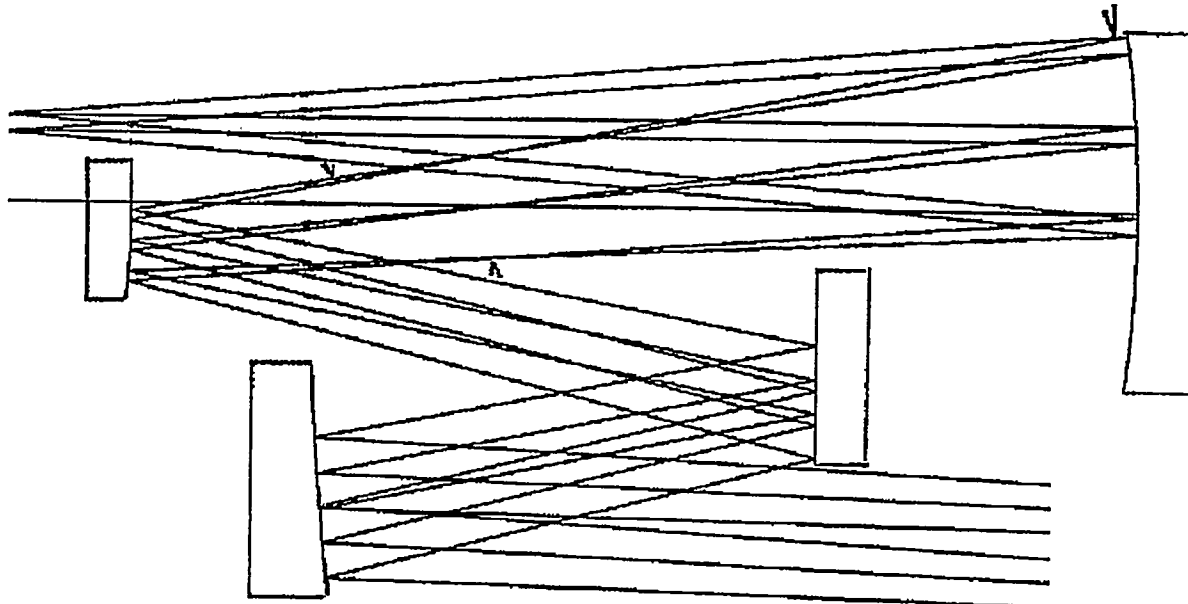


Figure 3. Large Etendu (n.a. = 0.085 camera).

This camera family was designed in two steps. First, a design space was identified using spherical mirrors only. Next, mild aspheric terms were added to tune the image quality and distortion for various ring-field widths. The design space was found using a unique Seidel-aberration-based merit function. The final design of each member in the camera family was done with standard ray-tracing techniques and a special distortion function.

The cameras must be nearly diffraction-limited at 13 nm, so the mirrors must have sub-nanometer surface figure accuracy. This requires interferometry of this same caliber — which can be done on mirrors with aspheric departures less than 2 microns. So, in these cameras, less asphericity is better, hence the all-spherical beginning.

Using Seidel aberrations in the first phase of this optimization allows us to concentrate on the aberration types that can best be controlled with mirror curvatures and spacings: Petzval curvature, distortion, and higher order astigmatism and coma. We lightly control the rest, knowing that we can null them later with mild aspherics.

The Seidel aberration expansion can be specialized so it emphasizes the aberrations in a ring field. For this, a Taylor expansion is written for each aberration type, centered in the ring field. For example, Petzval curvature can be written as:

$$Petzval(\alpha) = F(1) + \alpha \cdot \partial F(1)/\delta\rho + \alpha^2/2 \cdot (\partial\rho)^2 F(1)/(\delta\rho)^2 + \dots \quad (5)$$

where  $\rho$  is the normalized radius of the ring field,  $\alpha = \rho - 1$ , and the Seidel expansion for Petzval curvature is<sup>5</sup>:

$$F(\rho) = PZ3 \cdot \rho^2 + PZ5 \cdot \rho^4 + \dots \quad (6)$$

The derivatives of (6) at a radius  $\rho = 1$  are:

$$F(1) = PZ3+PZ5 \quad (7); \quad \partial F(1)/\partial \rho = 2 \cdot PZ3+4 \cdot PZ5 \quad (8); \quad \text{and} \quad \partial^2 F(1)/(\partial \rho)^2 = 2 \cdot PZ3+12 \cdot PZ5 \quad (9).$$

Equation (7) describes a constant focal shift which is unimportant. The first derivative term in Equation (8) describes the cone angle of the focal plane which should be nulled. The second derivative, Equation (9), is less important but should be minimized. Controlling these two terms "flattens" the widest possible ring field.

When the all-spherical design was completed (including control of other aberrations), a ray-based merit function was used to minimize the rms wavefront errors at five radii across the ring field. The distortion was minimized as follows: a change in distortion is a change in the camera's magnification, so the magnification was calculated at the five field points and the differences were minimized. Aspheric terms on the mirrors up to  $\rho^{12}$  were needed to achieve high image quality.

Three camera designs are presented in Table 1, all with minimal distortion and very good image quality. Two have numerical apertures of  $na = 0.1$  for printing 100-nm features over ring-fields with widths of  $\Delta r = 2 \text{ mm}$  and  $\Delta r = 2.6 \text{ mm}$ . The third has a smaller numerical aperture,  $na = 0.085$ , so it can print  $\approx 110\text{-nm}$  features. This allows a much wider ring field;  $\Delta r = 7 \text{ mm}$  which increases the Etendu to  $E_{camera} = 0.085 = 0.6 \text{ mm-sr}$ ; 6 times larger than the prior art.

TABLE 1. CAMERA PARAMETERS

Camera Features	>>> >>>	Small FOV High Strehl	Med. FOV	Less n.a. Large Etendu
Numerical Aperture		0.1	0.1	0.085
Ring-Field Width (mm)		2.0	2.6	7.0
Average Strehl Ratio (%)		99.2	97.5	98.0
P-P Distortion (nm)		18	24	13
Etendu (mm-sr)		0.2	0.26	0.6

**CONCLUSION:** Three new camera designs have been presented that will all allow more efficient use of the new debris-less laser-plasma sources. The best of these designs has an Etendu six times larger than any previous designs. A high-efficiency condenser<sup>2</sup> matched to this camera can collect 25% of the EUV radiated into  $4\pi$  steradians.

**ACKNOWLEDGEMENT:** This work was performed under DOE Contract DE-AC04-94AL85000.

## REFERENCES

<sup>1</sup> Unpublished work of G. D. Kubiak, D. O'Connell, and K. D. Krenz; SNL/CA.

<sup>2</sup> Sweat, U.S. Patent 5,361,292.

<sup>3</sup> T. E. Jewell and K. Thompson, U.S. Patent 5,315,629.

<sup>4</sup> Bruning, et al., US Patent 5,353,322.

<sup>5</sup> OSLO® Sinclair Optics, Inc., Fairport, New York.